Sonochemical characterisation of ultrasonic dental descalers **Revised manuscript**

Gareth J. Price*, T. Joyce Tiong[≠] and David C. King

Department of Chemistry, University of Bath, Bath, BA2 7AY, UK

Abstract

An ultrasonic dental descaling instrument has been characterised using sonochemical techniques. Mapping the emission from luminol solution revealed the distribution of cavitation produced in water around the tips. Hydroxyl radical production rates arising from water sonolysis were measured using terephthalate dosimetry and found to be in the range of μmol min^{-1}, comparable with those from a sonochemical horn. Removal of an ink coating from a glass slide showed that cleaning occurred primarily where the tip contacted the surface but was also observed in regions where cavitation occurred even when the tip did not contact the surface. Differences in behaviour were noted between different tip designs and computer simulation of the acoustic pressure distributions using COMSOL showed the reasons behind the different behaviour of the tip designs.

Keywords: sonochemiluminescence, cleaning, dental instruments, cavitation

Highlights

- Ultrasonic descaling instruments used in dentistry have been characterised by sonochemical methods
- Terephthalate dosimetry, luminol emission, surface cleaning show differences between different tip designs
- Cavitation can promote 'non-contact' removal of material from a solid surface
- Computer simulation of the acoustic pressure distributions explains in part the effect of size and shape of the descaler tips.

[≠] Present address: Department of Chemical and Environmental Engineering University of Nottingham, Malaysia, Jalan Broga, 3500 Semenyih, Selangor, Malaysia

INTRODUCTION

Ultrasonic instruments are widely used in dentistry for a range of drilling, cutting and cleaning operations [1]. A particular example is the ultrasonic descaler [2], used to remove deposits of calculus and other adherent materials from teeth around the gumline. A metal (usually titanium) tip, for which various designs are available, is mounted in a handpiece and vibrates at ultrasonic frequencies. The side of the free end of the tip is placed against the tooth, mechanically removing deposits on the surface. An irrigant, usually water or a dilute solution of sodium hypochlorite, passes over the tip to both reduce heating and wash away debris [3].

One mechanism which may assist in the cleaning is cavitation which could be generated in the irrigant solution adjacent to a tooth surface [4, 5]. This suggestion was reinforced by the detection by Lea *et al.* of transient cavitation generated by the vibratory motion of the scaler tips [6]

Cavitation occurs in liquids when the acoustic pressure during the rarefaction phase of an oscillation becomes more negative than the saturated vapour pressure of the liquid, leading to the formation of cavities or bubbles [7 - 9]. Cavitation results in both chemical and mechanical effects. The former include the formation of excited states with consequent light emission and reactive free radical species from pyrolysis of the liquid and any dissolved species. Examples of mechanical effects are acoustic streaming and the formation of microjets that impact on a solid surface adjacent to collapsing cavities.

Previous work [10, 11] showed that acoustic cavitation could be produced around descalers and that its spatial distribution depended in detail on the design of the tip; three different designs were found to give markedly different patterns of cavitation. The degree of cavitation, determined by using sonochemiluminescence from a luminol solution, was correlated with the vibratory motion of the tips characterised by scanning laser vibrometry, SLV, which measures motion of an object by monitoring the Doppler shift of a reflected laser beam. There was good correlation between the vibration amplitude at points along the tip and the observed sono-chemiluminescence with high levels of cavitation occurring at vibration antinodes. The exception was that minimal cavitation was found at the free end of the tip even though it was the point with maximum displacement. In order to optimise the cleaning efficiency of descaler tips and to facilitate further development of their design, it is necessary to have a better understanding of the effects caused by the tip motion. In this work, we apply a number of methods used to characterise sonochemistry systems to dental descaling equipment and present further results investigating the physical effects arising around the tips. To explain differences in their behaviour we use numerical simulation to predict the pressure fields and

hence likelihood of cavitation from the motion around the tips.

EXPERIMENTAL

Materials

All reagents were analytical grade and obtained from Sigma-Aldrich Co., UK, unless otherwise stated, and were used as received. The water used to prepare solutions was deionised water from a MilliQ system and had a resistance > 10 MΩ.

Dental descaler and calibration

The descaler used was a miniMaster Piezon descaler provided by Electro Medical Systems, Nyon, Switzerland which was used with three tips (labelled as 'A', 'P' and 'PS') having varying shape and size as shown in Figure 1. The ultrasound generator operates at a nominal frequency of 30 kHz, and was adjustable over a range of ten incremental power settings; these were calibrated for ultrasound intensity using the calorimetric method in the usual way [12]. A setting of 10 represented full power and was equivalent to 4.9 W, 6.8 W and 4.4 W for the 'A', 'P' and 'PS' tips respectively.

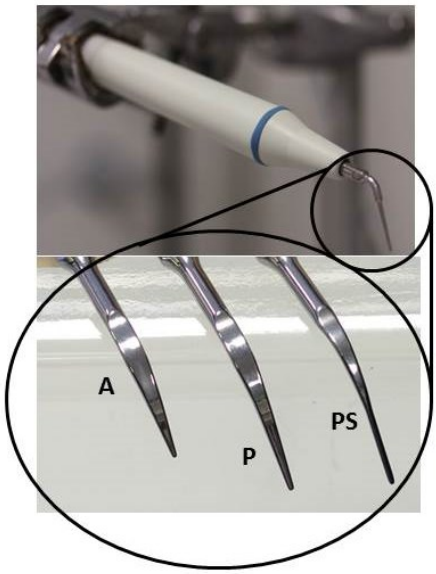

Figure 1. Descaler handpiece and tips. The three tips have lengths: A 12.3 mm; P 15.2 mm; PS 17.1 mm.

Cavitation Analysis

The degree of cavitation and its spatial distribution were measured by recording sonochemiluminescence emission [13]. A solution of luminol was prepared by dissolving 177

mg (1 mmol) of luminol (3-aminophthalhydrazide, 97%), 0.1 mol hydrogen peroxide and 0.1 mol EDTA (ethylenediaminetetraacetic acid, sodium salt) in 1 dm^3 of 0.1 mol dm^{-3} aqueous sodium carbonate. The solution was adjusted to pH 12 by adding sodium hydroxide. Images were recorded for 30 s on a Canon EOS 30D digital SLR camera or an Artemis ICX285 CCD camera, using a macro lens of 60 mm focal length at an aperture of f2.8, focusing on the dental instrument in order to obtain a 1:1 image ratio. The total intensity of the emission was calculated after subtraction of background levels using ImageJ software [14] which was also used for further image manipulation over a fixed region of interest.

Hydroxyl radical production was quantified using terephthalic acid dosimetry [15] by recording fluorescence spectra with a Perkin Elmer 4300 fluorimeter using excitation and emission wavelengths of 310 nm and 425 nm respectively. A 0.002 mol dm^{-3} solution of terephthalic acid in 0.005 mol dm^{-3} sodium hydroxide buffered to pH 6-11 with non-fluorescent phosphate buffer solution was contained in a 5 cm^3 quartz cuvette and the descaler mounted to ensure that the tip was immersed but did not contact the walls of the cuvette. The emission was measured after one minute operation at the chosen power and the procedure was repeated with fresh solution used for each measurement. Measurements were repeated with the tip held in contact with a section of glass microscope slide contained within the cuvette.

The fluorimeter was calibrated with a sample of 2-hydroxyterephthalic acid synthesised from 2-bromoterephthalic acid and sodium hydroxide [16] and purified by repeated reprecipitation from basic solution. The structure was confirmed by ^{13}C NMR spectroscopy and mass spectrometry. A 1×10^{-5} mol dm^{-3} solution of HTA was prepared in deionised water and the emission recorded. Successive dilutions were carried out to calibrate the spectrometer.

Cleaning and Surface erosion

A glass microscope slide was coated on one side with two layers of waterproof black ink from a permanent marker and allowed to dry. The slide was placed in front of a sheet of plain white paper and photographed with a Leica M8 digital camera and Leica 90 mm f /4 Macro-Elmar-M lens set to maximum magnification. It was clamped in place so that it was immersed in water and a descaler tip placed against the slide in various configurations. After operation for 5 minutes the slide was dried and rephotographed under the same conditions as above. Analysis of the images allowed an estimate of the area of ink removed by the descaling treatment.

The principal mineral component of tooth is hydroxyapatite, $Ca_{10}(PO_4)_6(OH)_2$. It is widely used in orthopaedic surgery for filling bone cavities. The material properties of

hydroxyapatite are similar to tooth enamel. Hydroxyapatite pellets were prepared [17] with a 1 cm diameter and immersed in fresh deionised water. A descaler tip was positioned to make contact between the centre of the pellet and point of the tip and operated at maximum power for 5 min. The pellets were dried and contact profilometry was performed with a Dektak 6M profilometer, from by Veeco Instruments Ltd., Cambridge, UK. The pellet was placed flat on the measurement platform and the stylus drawn across the surface and the surface profile recorded with a specified contact 'force' equivalent to between 1–50 mg. Although the clinical exposure for a tooth surface is up to around 30 seconds for a single treatment, a significantly longer duration was used here as it was anticipated that non-contact experiments would show significantly less erosion than measurements with the tip in contact with the sample. Scanning electron microscopy was conducted using a JEOL SEM6480LV microscope.

RESULTS AND DISCUSSION

Detection and measurement of cavitation

The potential for cavitation to benefit cleaning processes could arise from chemical or mechanical effects produced by sonication – or a combination of both. Hence in this work, measurements depending on each category were performed.

If chemical effects are important in cleaning, it is likely that these will depend in large part on hydroxyl radicals, OH•, the most strongly oxidising species formed ($E°$ = 1.77 V) and other highly oxidising species such as superoxide which arise from subsequent reaction of OH•. Hydroxyl radical production around dental descalers has been reported [10, 11] but this was conducted with the descaler tips immersed in luminol solution. In clinical use, the descaler will often be used in air around or in contact with teeth. To confirm that radicals are produced from potential cavitation under these circumstances, radical production under both conditions was measured. Firstly, the handpiece was clamped so that the tip was immersed in luminol solution contained in a 3 cm × 3 cm quartz cuvette; no irrigant was passed through the tip. In a separate series of experiments, the cooling water supply to the tip was replaced by luminol solution and the descaler operated in air to simulate clinical practice. The irrigant (or luminol solution) emerged from an orifice behind the tip as shown in Figure 2 at a flow rate of 65 cm^3 min^{-1}, the maximum available on the descaler unit used. Photographs were recorded using 30 s exposure with the descaler at full-power and are also shown in Figure 2.

These images confirm that hydroxyl radicals can be produced in the flow of irrigant when the descalers are operated in air. There are some differences in the pattern of cavitation

from when the tips are immersed in solution. In the latter case, sonochemiluminescence it is strongly localised to the region close to the descaler tip. The luminescence intensity is lower at the handpiece end of the tip and increases along its length. Luminescence is also observed near the free end of the tips in contrast to the observations in solution. When operated with the tip immersed in solution, emission is confined to particular regions along the length which, as previous work showed [10] correspond to the regions of maximum vibration.

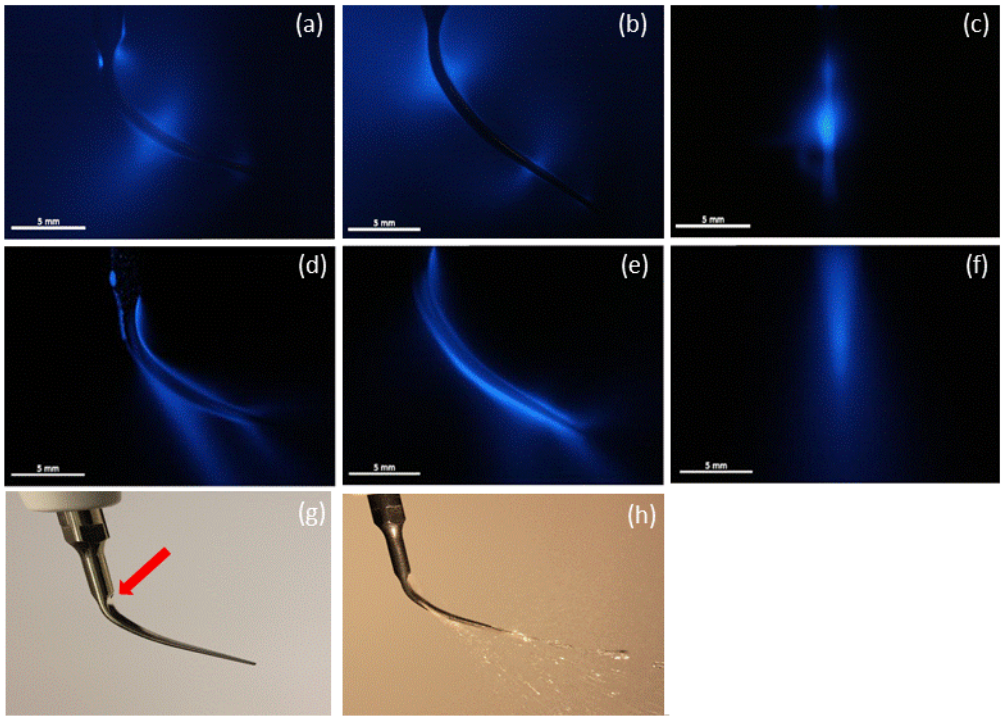

Figure 2. Luminol mapping of cavitation around descaler tips; 30 s exposure at full power. Tips immersed in solution (a) A tip; (b) P tip; (c) PS tip; tips in air with luminol irrigant flow (d) A tip; (e) P tip; (f) PS tip. PS tip is shown with a face-on orientation; (g) shows the configuration of the tip in air with the irrigant outlet indicated by the arrow; (h) illustrates the flow of the irrigant.

The results for the 'A' and 'P' tips are broadly similar although the volume over which luminescence is observed is more closely associated with the tip surface in the latter. It should be noted that no luminescence was observed when the ultrasound was switched off so that emission does not arise from hydrodynamic effects or from reaction with the metal surface. With the narrower 'PS' tip, the spray ejected from the underside shows none of the directional bias of cavitation activity to the left or right of the tip, which was visible in the solution-based measurements.

Emission was monitored over long exposure photographs and so integrates the luminescence over this period. The production of OH• and its escape from the bubble to react with luminol occurs over the course of a few microseconds and the lifetime of the luminol excited state is short, having been reported as 10 ns [18]. The flow rates used are sufficient for the luminol solution to flow only a short distance (< 1 mm) along the length of the tip so that it does seem that cavitation is being produced along the length of the tip and can therefore potentially play a part in cleaning ([19]). It has been suggested that such an aerosol may disperse microorganisms when a descaler is used in vivo [20]. Such cavitation could help to disinfect the cleaned areas as well as promoting cleaning.

While the emission from luminol is useful in confirming whether and where cavitation takes place, it is difficult to extract quantitative results. In order to measure the concentrations of OH• the terephthalate dosimeter (Scheme 1) was used. Figure 3 shows the rate at which radicals are trapped when the tips were operated at full power. Experimental considerations meant that this was performed with the tip immersed in the terephthalate solution although removed before analysis. There was a linear dependence of radical production with time although the rates, shown in Table 1, were different for the different tip designs confirming previous observations [10]. The levels of radical production are comparable [15] with those produced by a typical 20 kHz sonochemical horn, albeit in a smaller volume of solution than would normally be involved.

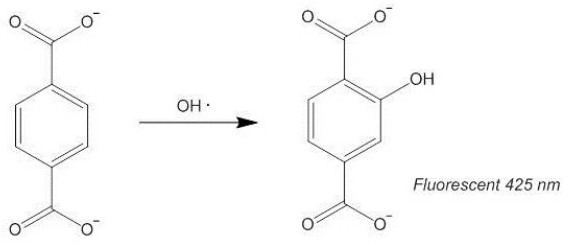

Scheme 1

Table 1. Rate of OH• radical production ($\times 10^{-6}$ mol $dm^{-3}min^{-1}$) during operation at full power of descaler tips free in solution and in contact with a glass slide.

Tip	Free solution	Contact
A	0.37	0.15
P	0.39	0.17
PS	0.28	0.11

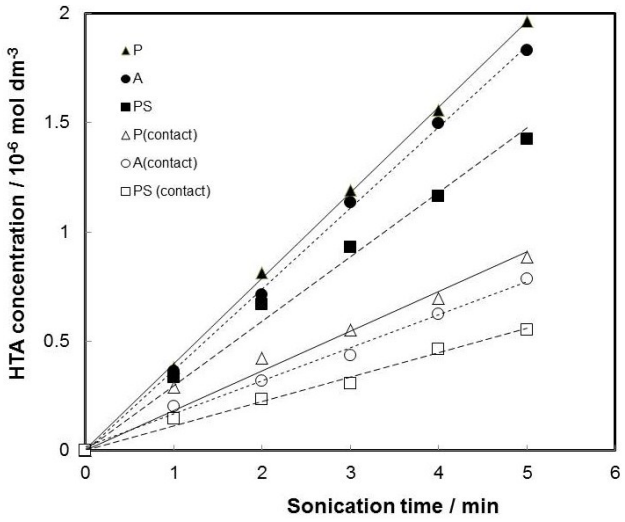

Figure 3. Production of OH radicals monitored by terephthalate dosimetry. The descalers were operated at full power; 'contact' signifies that the tips were placed against a glass slide.

Placing the descaler tip in contact with a glass slide to mimic contact with a solid surface such as a tooth, reduces the radical production rate by over half (Table 1). It was recently shown [11] that the amplitude and pattern of the vibratory motion of the tip was modified on contact so that the positions of maximum cavitation moved along the tip and the overall levels were reduced. This has significance in the clinical context since reducing cavitation and hence OH• radicals could limit any beneficial effects in cleaning or disinfecting during treatment.

Surface erosion and cleaning

Evaluation of cleaning performance is complicated by the lack of a standard method for evaluating the efficiency, although there are standards for descaler design and operation [21]. Previous work by Walmsley *et al.* [5] observed erosion of a simulated dentine surface placed in the path of cooling water from an operating descaler tip. A related approach with a different style of ultrasonic dental instrument was used by van der Sluis and co-workers [22]. In our work, surface profilometry and electron microscopy of treated hydroxyapatite pellets was performed to assess effects on a surface. However, reproducible quantitative information was difficult to obtain so an alternative was devised whereby a microscope slide was coated with black ink, which could then be removed by the descaler. The eroded area was determined by photography before and after treatment so as to determine the optimum conditions for ink erosion.

Initial experiments involved the tip in the configuration shown in Figure 4 where the tip was in contact with the slide. As expected, ink was removed from the area in contact but with the A tip, significant removal was also seen near the centre of the tip even though there was no contact. This corresponds to the region of the tip where cavitation is maximised [10, 11]. However, this was only noticed for this tip; no such removal in regions with no contact was seen with the other two tips investigated as shown in Figure 5 (a) although ink was removed around the point of contact. A summary of the relative performance of the three tips is given in Table 2.

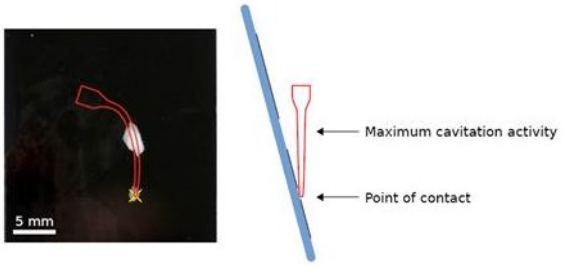

Figure 4. Removal of ink from a coated microscope slide. 'A' tip operated in water at full power for 5 min.

Changing the configuration so that the central region of the tip was in contact with the slide gave results typified by those in Figure 5(b). A larger amount of ink was removed and there was only a small difference between the three tips. In order to assess the viability of using the cavitation produced as a 'non-contact' cleaning method, a third configuration was adopted where the tip was placed parallel to the slide at a fixed distance of 1 mm. As can be seen in Figure 5(c) some removal was seen for tip A, comparable to that removed while in contact, but not for the other tips. This suggests that, with the appropriate design of tip which would optimise cavitation, cleaning without direct contact should be possible.

To assess the effects and possible damage that cleaning could have, the A tip (having shown the largest radical production and ink removal) was used with a hydroxyapatite pellet. No effect on the surface was observed under clinically reasonable conditions but to exaggerate possible changes to the surface, the tip was operated at full power for 15 min while immersed in water. The results when the tip was in contact using the same configuration as shown in Figure 4 are shown in Figure 6. The point of contact is marked by a pronounced indentation and darkening of the surface. Also of significance is an area around the mark which is lighter in appearance than the untreated surface; this corresponds to an area over which luminol mapping indicates that cavitation occurred. Looking at the surface in detail, the hydroxyapatite grown

under the conditions used here appears rough at high magnification. However, it is clear from comparing Figures 6(b) and 6(d) that the descaling treatment debrides some of the surface roughness and leaves a smoother surface where contact was made. The area around the contact region was relatively unaffected. To gain a measure of the debridement, surface profilometry was performed with the results shown in Figure 7. The indentation caused by tip contact is around 10-12 μm deep and around 150 – 200 μm in width.

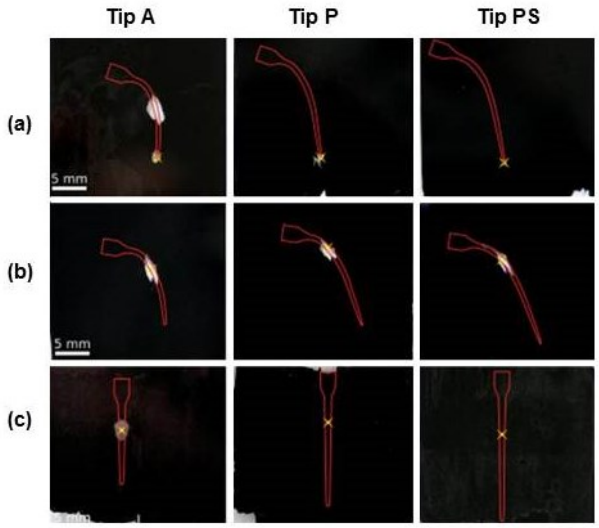

Figure 5. Removal of ink from a coated microscope slide for three tips operated in water at full power for 5 min. (a) end in contact with slide (see Fig. 4); (b) centre of tip in contact; (c) centre of tip 1 mm from slide.

Table 2. Areas of erosion areas for 'A', 'P' and 'PS' dental tips

Tip	Orientation	Eroded area / mm^2
A	End in contact	7.2
P		1.3
PS		0.3
A	Centre in contact	4.3
P		3.3
PS		3.7
A	Centre, 1 mm away	4.5
P		0
PS		0

Given the removal of ink from a slide by ‘non-contact’ treatment described above, a hydroxyapatite pellet was treated under the same conditions with the tip mounted 1 mm from the surface. Figure 8 shows that operation in this configuration has broadly similar effect on the surface. The electron micrographs show a similar flattening of the surface although the profile shows that the indentation is not as deep and the effects are distributed over a wider area than when the tip was in contact. Contact with the surface reduces the amount of cavitation produced [11] which is consistent with the observations here and the erosive abilities of cavitation occurring around ultrasonic descalers are reduced when a tip is in contact with a hard surface, and that physical contact dominates the erosion process.

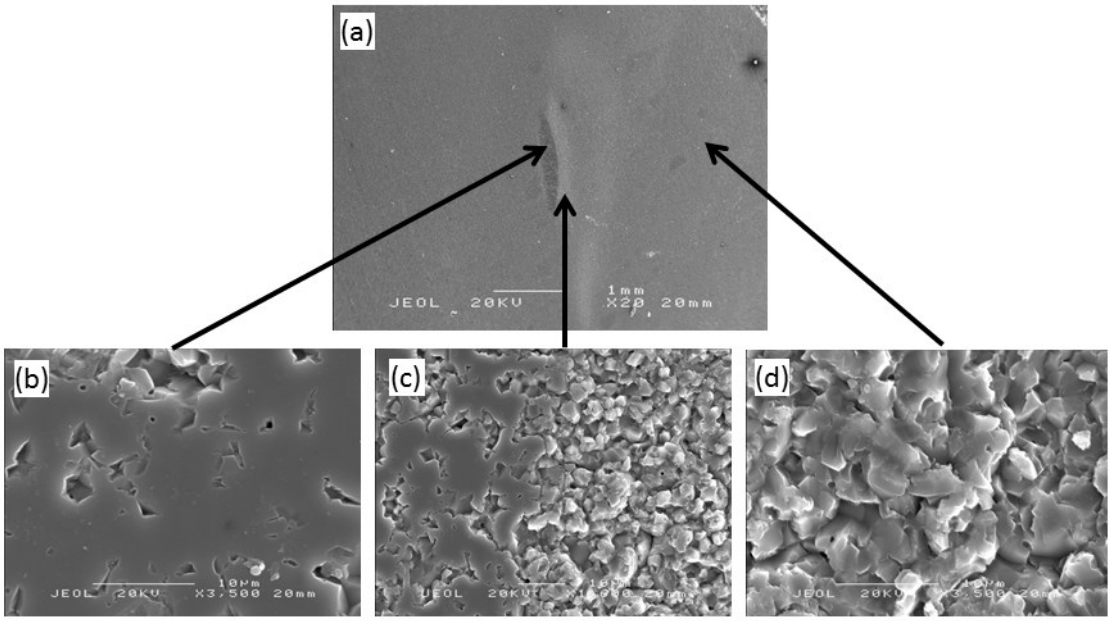

Figure 6. Scanning electron micrographs of hydroxyapatite after 15 min contact with tip A operating at full power (a) magnification × 20; (b) contact area, magnification × 3500; (c) boundary of contact area, magnification × 500; (d) untreated area, magnification × 3500.

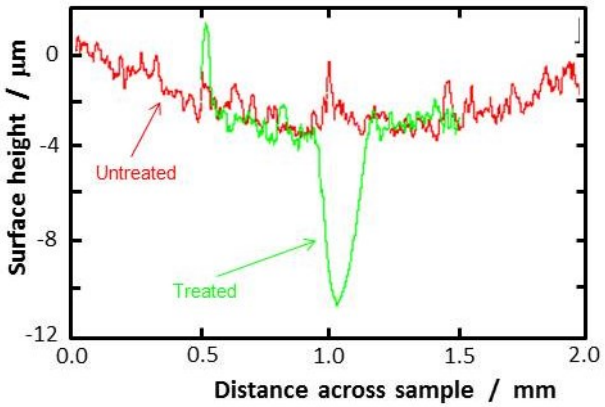

Figure 7. Surface profilometry of hydroxyapatite disks before and after 15 min contact with tip A operating at full power in water.

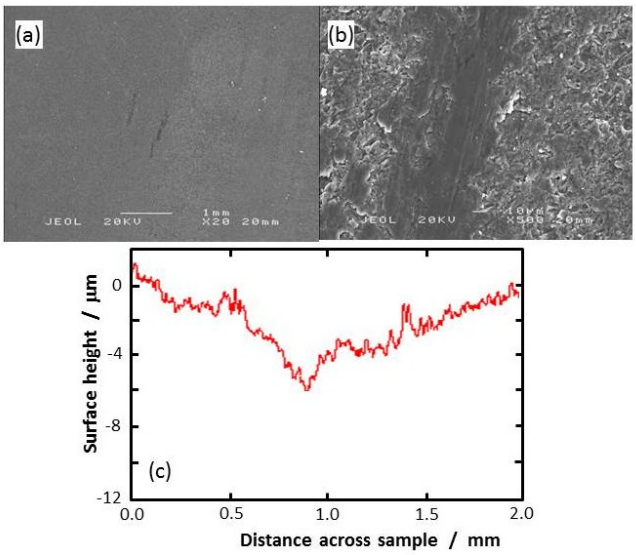

Figure 8. Scanning electron micrographs of hydroxyapatite after 15 min treatment with tip A operating at full power 1 mm away from surface (a) magnification × 20; (b) modified area, magnification × 500; (c) Surface profilometry of hydroxyapatite disks.

Influence of tip design

It is clear from these results that each of the descaler tips can remove a coating from a hard surface. However a complete characterisation of their action demands an understanding of why the different designs cause different effects.

One possibility is that, even though the nominal input power is the same in each case, the ultrasound intensities generated may be different. In the results presented here, each tip was operated at a setting of 10 on the dial *i.e.* full power. The power generated by the tip was measured calorimetrically [12] by measuring the temperature rise with time of a known volume

of water which had been calibrated with an electrical heater. The emitting areas were estimated from magnified photographs of the tips adjacent to a calibration. The results are shown in Table 3 and indicate that, while the output intensities are similar, there are significant differences between the tips. The lowest intensity is for the PS tip, which correlates with the lower levels of radical production reported above. The comparison of the A and P tips is complicated by their different areas. The latter outputs more power, which correlates with the radical production rates in Table 1, while the smaller area of the A tip results in higher intensities, which correlates with the cleaning results in Table 2. These results add further weight to the argument that the detailed size and shape of the tips is important in determining their performance.

Table 3. Calorimetric determination of ultrasound intensity at full generator power.

Tip	Area / cm^2	Power / W	Intensity / W cm^{-2}
A	0.31	4.9	15.8
P	0.45	6.8	15.1
PS	0.31	4.4	14.2

It is tempting to speculate on potential shape and size effects. Both the A and P tips are broad with respect to the thickness of the tip whereas the PS tip is narrower and rounded (see Figure 1). This may mean that the PS tip moves more smoothly through the water and so cannot produce sufficiently negative pressures to generate high levels of cavitation. Conversely, the broader tips will be able to move larger volumes of liquid and hence generate higher negative pressures behind the motion. In order to further investigate this influence, we turned to computer modelling.

Computer simulation or acoustic pressure fields

Computational modelling has been used on a number of ultrasonic systems to predict the behaviour. Of relevance to the current work is the use by Klima *et al.* [23] and Raman *et al*. [24] of finite element analysis modelling applying the COMSOL Multiphysics™ package to predict the intensities and acoustic pressures around a 20 kHz ultrasonic probe. Torres-Sánchez and Corney used the method to predict the acoustic fields in a reactor used to produce polymer foams [25].

The principle here is to apply the modelling to predict the acoustic pressure fields in water surrounding the operating tip having inputted the details of the tip shape, material

properties, oscillation frequency and pattern from the vibrometry [10]. While the exact occurrence of cavitation cannot be predicted directly, it will occur where the acoustic pressure exceeds a threshold value so that, to a reasonable approximation, areas of cavitation would be expected to correspond to the areas with highest acoustic pressure. The precise acoustic pressure needed to produce cavitation is difficult to define as it depends on a large number of factors such as frequency, temperature and the nature of the liquid. For ultrasound frequencies around 20 kHz at room temperature, estimates range from 0.1 MPa for air saturated water to 18 - 20 MPa for highly degassed water. [26, 27]

Simulations were performed using the pressure acoustics frequency domain in COMSOL Multiphysics 4.3 using literature values of the relevant variables such as the density of, and speed of sound in, water. The methods and verification of the models used have been described elsewhere [28]. Briefly, the geometry of the tip was carefully measured and inputted into the model. A simulated oscillation of the appropriate frequency was applied to the tip and the acoustic pressure emitted into the surrounding water was calculated.

The distribution of acoustic pressure in the water around the tip is found by solving the wave equation, Equation (1). Here, it is assumed that wave propagation is linear and shear stress is neglected, i.e. water is treated as incompressible.

$$\frac{1}{\rho_o c^2}\frac{\partial^2 p}{\partial t^2} + \nabla\left(-\frac{1}{\rho_o}\nabla p\right) = 0 \qquad (1)$$

where ρ is the density of the liquid and c the speed of sound. The pressure, p, as a function of distance varies with the oscillation frequency, ω according to

$$p(r,t) = p_o(r)e^{i\omega t} \qquad (2)$$

leading to the Helmholtz equation

$$\nabla\left(-\frac{1}{\rho_o}\nabla p\right) - \frac{\omega^2}{\rho_o c^2}p = 0 \qquad (3)$$

Which can be solved using suitable boundary conditions, in this case that the edge of the descaler tip was a hard boundary so that $p = p_o$ and $\frac{\partial p}{\partial r} = 0$, where p is the acoustic pressure and n is the normal vector to the boundary surface. The air-water interface and the walls of the container were treated as totally reflecting. COMSOL performs finite element analysis based on meshes generated around domains. For this study, a predefined tetrahedron mesh was used.

The pressure amplitude, p_o, was calculated from the acoustic intensity, I, using

$$I = \frac{p_o^2}{2\rho c} \tag{4}$$

The simulation results for the three tips are shown in Figures 9 and 10. The absolute values of the pressures generated are rather lower than might be expected to lead to significant levels of cavitation. There are approximations involved in the simulations and a number of factors such as acoustic streaming and any interaction with a cloud of cavitation bubbles are not included. However, the focus here is on the relative pressures in different regions around the oscillating tip and this consideration does allow conclusions to be drawn. Looking at the side-on views in Figure 9a, the simulated pressure distribution is compared with the production of cavitation as shown by emission from a luminol solution. For the A tip, the highest pressure differences are generated from about half-way along towards the free end. While the agreement is not perfect, the brightest luminol emission occurs from a similar region. Perhaps of more importance, the pressure distribution around the P tip is very different with the highest values being generated around the bend together with a smaller region at the end; this correlates well with the luminol emission. The simulated distribution around the PS tip is similar although it extends over a smaller region near the bend of the tip. Similar remarks can be made on the front-on views of the tips in Figure 10, in this case compared with the observed cloud of cavitation bubbles [10]. Again, cavitation is concentrated into a single region for the A tip while for the P tip there are two regions of bubbles and high pressure differences. The simulated pressure distributions for the P and PS tips are similar although the former extends over a larger region, as reflected in the experimental results. These simulations add additional evidence to the suggestion that the narrower, more rounded shape of the PS tip lead to cavitation being generated over a small region.

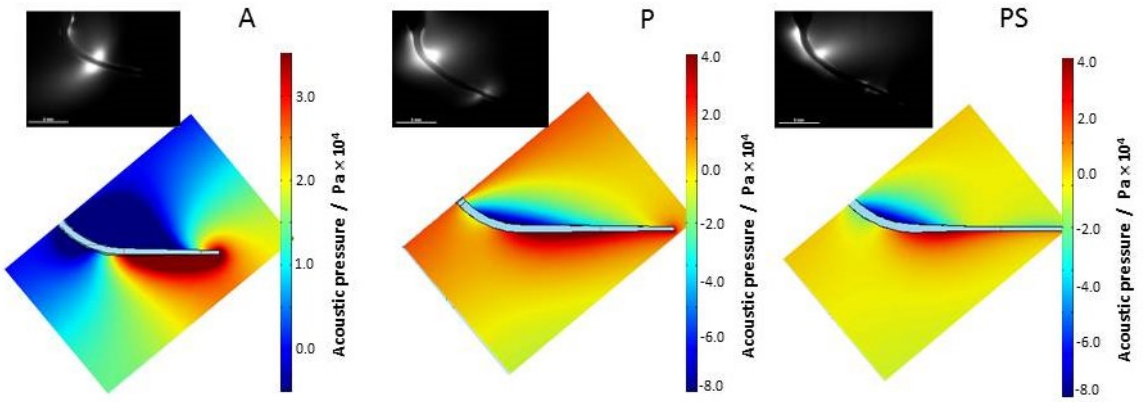

Figure 9. Simulation of acoustic pressure generated by descaler tips operating at full power in water. Insets show photographs of luminol emission

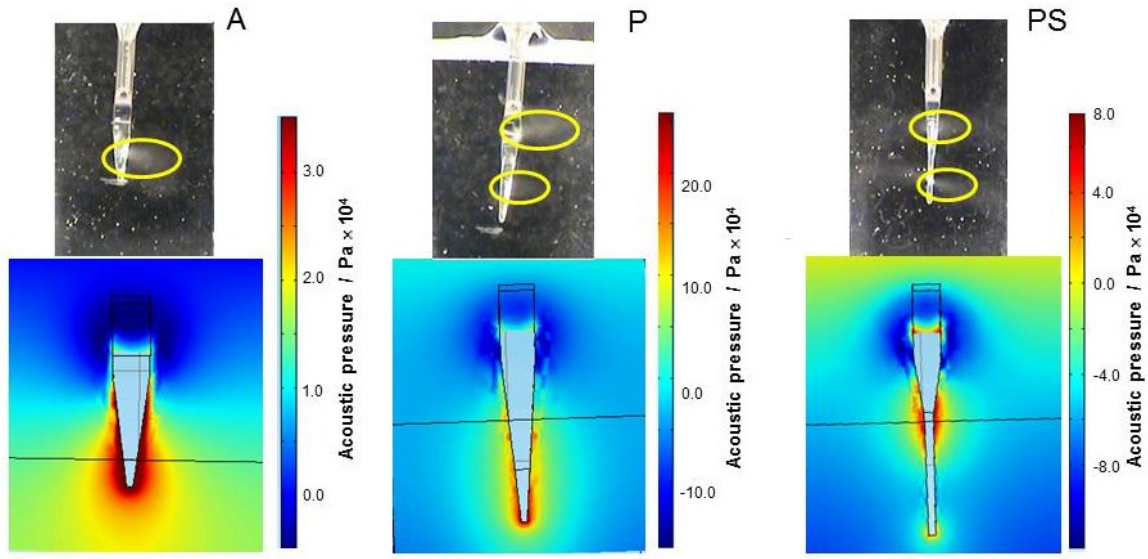

Figure 10. Simulation of acoustic pressure generated by descaler tips operating at full power in water. Insets show photographs with visible cavitation bubble clouds circles.

CONCLUSIONS

A number of methods usually used to characterise sonochemical systems have been applied to ultrasonic dental descaling instruments and confirmed that significant levels of cavitation can be generated. The cavitation can assist in the cleaning process of the descalers. Both the level and spatial distribution of cavitation depend on the precise shape and size of the tip. Computer simulation showed that this is due to the tip design generating different acoustic pressures around the tip. The work shows that changing the design markedly affects the cleaning efficacy and so will allow further developments in tip design and optimisation of their behaviour.

ACKNOWLEDGEMENTS

We gratefully acknowledge the Engineering and Physical Sciences Research Council for funding *via* grants EP/C536908/1 and EP/ F021739/1 as well as useful discussions with Professor Damien Walmsley of the University of the Birmingham School of Dentistry. We would also like to acknowledge the loan of a Piezon miniMaster ultrasonic descaler and set of tips by Electro Medical Systems and Prof S. T. Kolaczkowski for the use of the COMSOL simulation programme.

REFERENCES

1. AD Walmsley, SC Lea, G Landini, AJ Moses Advances in power driven pocket/root instrumentation J. Clin. Periodontol. **35** (2008) 22-28
2. J Tunkel, A Heinecke, TF Flemming, A systematic review of efficacy of machine-driven and manual subgingival debridement in the treatment of chronic periodontitis J. Clin. Periodontol. **29** (2002), 72–81
3. LWM van der Sluis, M Versluis, MK Wu, PR Wesselink, Passive ultrasonic irrigation of the root canal: a review of the literature Int. Endodont. J. **40** (2007) 415-426
4. AD Walmsley, WRE. Laird, AR Williams, A Model System to Demonstrate the Role of Cavitational Activity in Ultrasonic Scaling J. Dent. Res. **63** (1984), pp. 1162–1165.
5. AD Walmsley, TF Walsh, WRE. Laird and AR Williams, Effects of cavitational activity on the root surface of teeth during ultrasonic scaling, J. Clin. Periodontol. 17(5), (1990) 306–312
6. SC Lea, GJ Price, AD Walmsley, A study to determine whether cavitation occurs around dental ultrasonic scaling instruments Ultrason. Sonochem. **12** (2005) 233–236.
7. TG Leighton: The Acoustic Bubble Academic Press, London, 1994.
8. M Ashokkumar and T Mason "Sonochemistry", Kirk-Othmer Encylcopedia of Chemical Technology, John Wiley & Sons, 2007
9. FR Young "Cavitation", Imperial College Press, London, 1999.
10. B Felver, DC King, SC Lea, GJ Price and AD Walmsley Cavitation occurrence around ultrasonic dental scalers Ultrason. Sonochem. 16, (2009) 692 – 697
11. AD Walmsley, SC Lea, B Felver, DC King and GJ Price Mapping Cavitation activity around dental ultrasonic tips Clin. Oral Invest. **17**, (2013) 1227 – 1234
12. S Koda, T Kimura, T Kondo, H Mitome, A standard method to calibrate sonochemical efficiency of an individual reaction system, Ultrason. Sonochem. **10**(3) (2003) 149–156.
13. GJ Price, NK Harris and AJ Stewart Direct observation of cavitation fields at 23 and 515 kHz Ultrason. Sonochem. **17** (2010) 30-33
14. MD Abramoff, PJ Magelhaes, SJ Ram, Image processing with Image J Biophotonics Intl. **11** (2004) 36 - 39.

15. GJ Price and EJ Lenz The use of dosimeters to measure radical production in aqueous sonochemical systems. Ultrasonics **31(6)**, (1993) 451-456

16. L Field and PR Engelhardt, Organic Disulfides and Related Sub- stances. XXX. Preparations and Reactions of Mercaptoterephthalic Acids and Derivatives J. Org. Chem. 25(11), (1970) 3647–3655

17. YH Hsu, IG Turner and AW Miles Fabrication of Porous Calcium Phosphate Bioceramics as Synthetic Cortical Bone Graft, Key Eng. Mat. (2005) 284-308.

18. M Voicescu S Ionescu On the Fluorescence of Luminol in a Silver Nanoparticles Complex J Fluoresc **23** (2013) 569–574

19. DG Offin, C Vian, PR Birkin and TG Leighton An assessment of cleaning mechanisms driven by power ultrasound using electrochemistry and high-speed imaging techniques. Hydroacoustics, **11,** (2008) 299-312.

20. DP Lu and RF Zambito Aerosols and cross infection in dental practice–a historic view General Dentistry 29(2), (1981) 136–142

21. "Ultrasonics - Dental descaler systems - Measurement and declaration of the output characteristics" Report IEC 61205 ed1.0, International Electrotechnical Commission 1993

22. LWM van der Sluis, MK Wu, PR Wesselink, The efficacy of ultrasonic irrigation to remove artificially placed dentine debris from human root canals prepared using instruments of varying taper Int. Endodont. J. **38** (2005) 764-768

23. J Klima, A Frias-Ferrer, J Gonzalex-Garcia, J Ludvik, V Saez, J Iniesta Optimisation of 20kHz sonoreactor geometry on the basis of computational simulation of local ultrasonic intensity and qualitative comparison with experimental results. Ultrason. Sonochem., 14**,** (2007) 19-28

24. V Raman, A Abbas and SC Joshi Mapping local cavitation events in high intensity ultrasound fields. Proceedings of the COMSOL Users Conference November 2006, Bangalore. 2006

25. C Torres-Sánchez, JR Corney Manufacture of graded porosity foams: Simulation of local ultrasonic pressure and comparison with experimental results, Proc. 20th Int. Congress on Acoustics 2010, Sydney, Australia

26. W.J. Galloway, An Experimental Study of Acoustically Induced Cavitation in Liquids, J. Acoust. Soc. Amer., **26** (1954) 849-857.

27. E. Herbert, S. Balibar, F. Caupin, Cavitation pressure in water, Phys. Rev. E **74** (2006) 041603 (1–22).

28. T.J. Tiong, Sonochemical and ultrasonic output analyses on dental endosonic instruments, PhD Thesis, University of Bath, United Kingdom., 2012, ; Manuscript in preparation.

CAPTIONS FOR FIGURES

Figure 1. Descaler handpiece and tips. The three tips have lengths: A 12.3 mm; P 15.2 mm; PS 17.1 mm.

Figure 2. Luminol mapping of cavitation around descaler tips; 30 s exposure at full power. Tips immersed in solution (a) A tip; (b) P tip; (c) PS tip; tips in air with luminol irrigant flow (d) A tip; (e) P tip; (f) PS tip. PS tip is shown with a face-on orientation; (g) shows the configuration of the tip in air with the irrigant outlet indicated by the arrow; (h) illustrates the flow of the irrigant.

Figure 3. Production of OH radicals monitored by terephthalate dosimetry. The descalers were operated at full power; 'contact' signifies that the tips were placed against a glass slide.

Figure 4. Removal of ink from a coated microscope slide. 'A' tip operated in water at full power for 5 min.

Figure 5. Removal of ink from a coated microscope slide for three tips operated in water at full power for 5 min. (a) end in contact with slide (see Fig. 4); (b) centre of tip in contact; (c) centre of tip 1 mm from slide

Figure 6. Scanning electron micrographs of hydroxyapatite after 15 min contact with tip A operating at full power (a) magnification × 20; (b) contact area, magnification × 3500; (c) boundary of contact area, magnification × 500; (d) untreated area, magnification × 3500

Figure 7. Surface profilometry of hydroxyapatite disks before and after 15 min contact with tip A operating at full power in water.

Figure 8. Scanning electron micrographs of hydroxyapatite after 15 min treatment with tip A operating at full power 1 mm away from surface (a) magnification × 20; (b) modified area, magnification × 500; (c) Surface profilometry of hydroxyapatite disks

Figure 9. Simulation of acoustic pressure generated by descaler tips operating at full power in water. Insets show photographs of luminol emission

Figure 10. Simulation of acoustic pressure generated by descaler tips operating at full power in water. Insets show photographs with visible cavitation bubble clouds circles.

TABLES

Table 1. Rate of OH• radical production ($\times 10^{-6}$ mol $dm^{-3}min^{-1}$) during operation at full power of descaler tips free in solution and in contact with a glass slide.

Tip	Free solution	Contact
A	0.37	0.15
P	0.39	0.17
PS	0.28	0.11

Table 2. Areas of erosion areas for 'A', 'P' and 'PS' dental tips

Tip	Orientation	Eroded area / mm^2
A	End in contact	7.2
P		1.3
PS		0.3
A	Centre in contact	4.3
P		3.3
PS		3.7
A	Centre, 1 mm away	4.5
P		0
PS		0

Table 3. Calorimetric determination of ultrasound intensity at full generator power.

Tip	Area / cm^2	Power / W	Intensity / W cm^{-2}
A	0.31	4.9	15.8
P	0.45	6.8	15.1
PS	0.31	4.4	14.2